

Theoretical interpretation of electronic absorption and emission transitions in 9-acridinones

A. Bouzyk^a, L. Józwiak^a, A.Yu. Kolendo^b, J. Błażejowski^{a,*}

^a Department of Chemistry, University of Gdańsk, Sobieskiego 18, 80-952 Gdańsk, Poland

^b Department of Chemistry, Kyiv Taras Shevchenko National University, 01033 Kiev, Volodymyrska 64, Ukraine

Received 4 January 2002; received in revised form 10 May 2002; accepted 13 May 2002

Abstract

Stationary absorption, fluorescence excitation and fluorescence spectra for 9(10*H*)-acridinone, 9(10-methyl)-acridinone, 2-methyl-9(10-methyl)-acridinone, 2-nitro-9(10-methyl)-acridinone, 9(10-ethyl)-acridinone and 9(10-phenyl)-acridinone dissolved in 1,4-dioxane, methyl alcohol or acetonitrile, as well as the available spectral characteristics reported by others were compared with those predicted theoretically at the semi-empirical PM3/CI (including the solvent effect within the COSMO model) or PM3/S levels of theory, in order to interpret spectral features of the compounds, i.e. the energies and probabilities of $S_0 \rightarrow S_n$, $S_0 \rightarrow T_1$, $T_1 \rightarrow T_2$, $S_1 \rightarrow S_0$, $T_1 \rightarrow S_0$ and $S_1 \rightarrow T_1$ transitions. Calculations at the PM3 and PM3/CI levels of theory enabled the structural changes accompanying $S_0 \rightarrow S_1$, $S_1 \rightarrow T_1$ and $T_1 \rightarrow S_0$ transitions to be investigated; they yielded, moreover, basic physicochemical characteristics of the molecules in the ground and excited electronic states. Theoretically predicted dipole moments and charge distributions in the S_0 , S_1 and T_1 states provided further insight into the nature of electronic transitions in 9-acridinones. The predicted characteristics correlate quite well with the available experimental ones, thus providing confirmation of the utility of theory in predicting the features of electronically excited molecules and interpreting the electronic transitions occurring in them.

© 2002 Elsevier Science B.V. All rights reserved.

Keywords: 9-acridinones; Electronic absorption and emission spectra (transitions); Theory; Interpretation; Features of excited states

1. Introduction

9-Acridinones are heterocyclic compounds containing secondary or tertiary amino and keto fragments within the ring system that confer on

these molecules the ability to interact specifically with other molecules from their immediate surroundings [1,2]. These compounds are therefore convenient models for investigating the features of entities that are at once aromatic amines and ketones. Of particular interest is the ability of 9-acridinones to absorb UV–VIS radiation and emit it efficiently in the short-wavelength visible region. The absorption of gaseous 9(10*H*)-acridinone and 9(10-methyl)-acridinone [3], the absorption of

* Corresponding author. Tel.: +48-58-3450331; fax: +48-58-3410357

E-mail address: bla@chemik.chem.univ.gda.pl (J. Błażejowski).

these compounds and their derivatives dissolved or dispersed in media of different polarities, and their ability to undergo specific interactions have been thoroughly investigated [4–17]. Numerous investigations have been focused on the photoluminescence [10,11,13,15,18–34] or chemiluminescence [15,35–40] of electronically excited 9-acridinones formed, in the latter case, during highly exothermic reactions of 9-substituted acridines with oxidants. The position of the fluorescence bands depends on the properties of the medium [10,11,20,24], the temperature [22,24,25], and the concentration of the emitting entities [25]. The

fluorescence quantum yield is close to unity in protic media, above 10% in specifically interacting polar media, and of the order of a few percent in neutral solvents such as aliphatic or aromatic hydrocarbons [20,22,28,29,32]. In relation to this, fluorescence lifetimes are of the order of nano or several nanoseconds, while phosphorescence lifetimes are measured in seconds [20,22,28,29,32]. It is ought to be mentioned additionally that not only $T_1 \rightarrow T_2$ absorption [17,21,22,26,30,41,42], but also the absorption [1,12,15,18,19,34] and emission [7,15,18,19,23,34] of anionic [1,7,15] and cationic [12,15,18,19,23,34] forms of 9-acridinones have

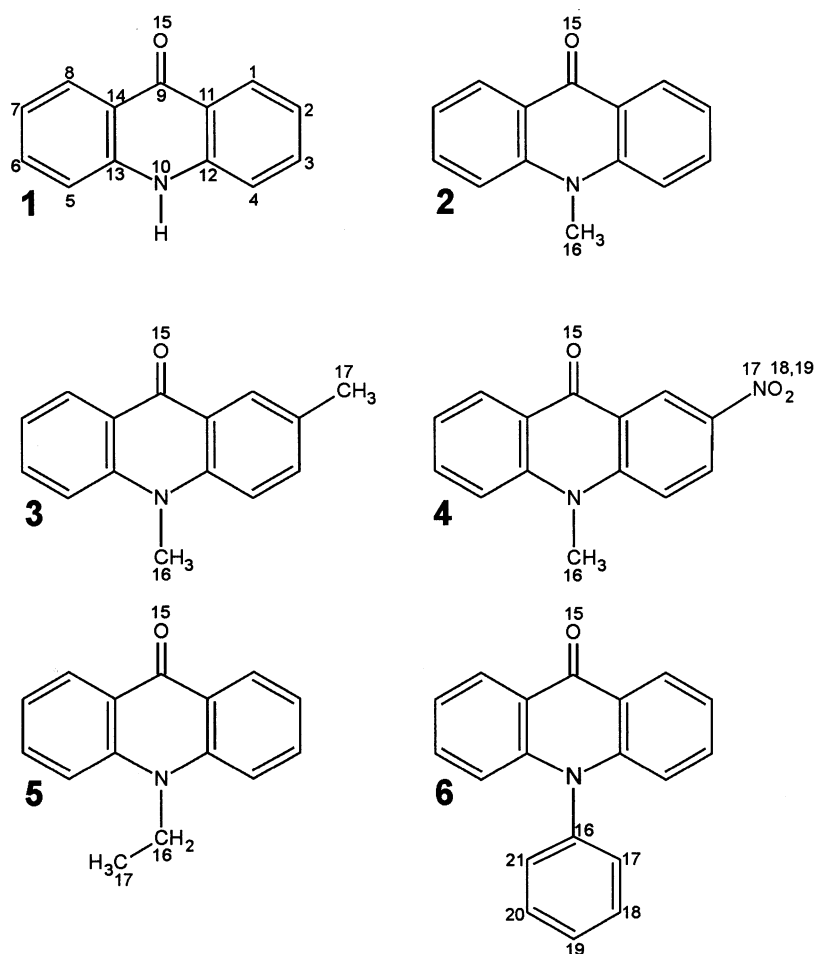


Fig. 1. The compounds investigated: 1—9(10*H*)-acridinone; 2—9(10-methyl)-acridinone; 3—2-methyl-9(10-methyl)-acridinone; 4—2-nitro-9(10-methyl)-acridinone; 5—9(10-ethyl)-acridinone; and 6—9(10-phenyl)-acridinone. The numbering of the atoms is indicated.

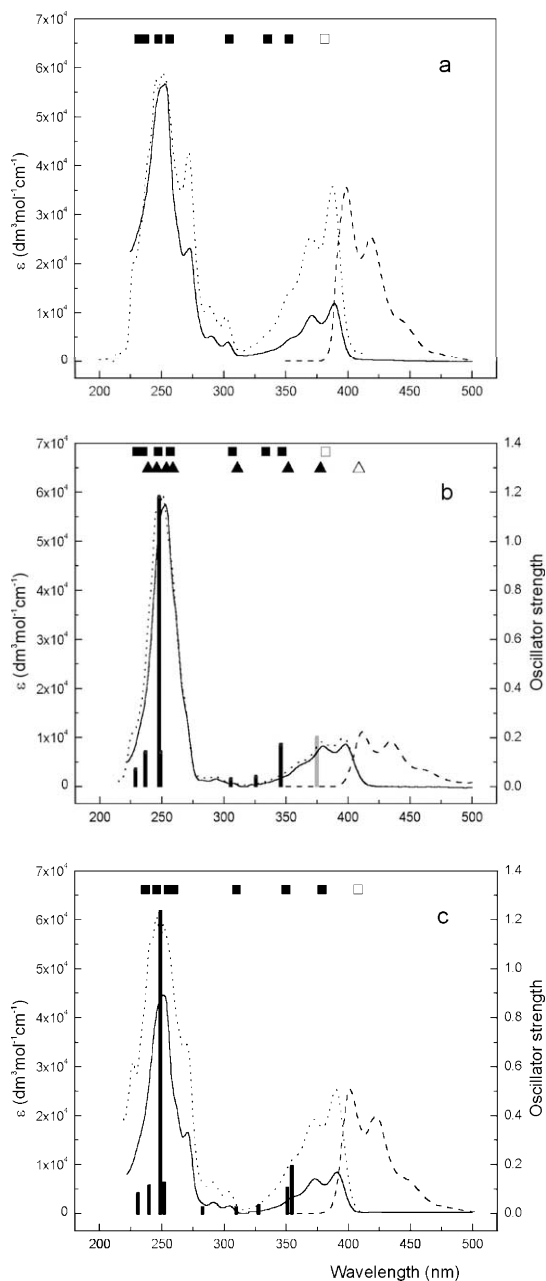


Fig. 2. Absorption (—), fluorescence excitation (.....) and fluorescence (----) spectra of **1** in 1,4-dioxane (a), CH₃OH (b) and CH₃CN (c), together with theoretically predicted excitation (■, ▲, ▣) and emission (□, △, ▢) transitions (values for the gaseous phase are represented by ▲ and △ in (b)). PM3/S, lower values; PM3/CI, higher values.

been investigated in the past. The above brief review leaves the impression that the electron

spectroscopy of 9-acridinones is quite well understood. This is indeed true with regard to our empirical knowledge of this subject. Theory, on the other hand, has been applied only sporadically. Thus, Sakhno et al. employed CNDO/S and INDO/S methods to predict the wavenumbers of electronic transitions in 9(10*H*)-acridinone [27], while Ishijima et al. calculated the energies of electronic transitions and oscillator strengths in this compound using PPP and CNDO/S methods with a view to interpret its MCD spectra [43]. SCF MO LCAO calculations with the solvent simulated by an external uniform electric field were also carried out by Korotkova et al. [33] and Sakhno et al. [44] in attempts to account for differences in the fluorescence spectra of 9(10*H*)-acridinone in polar and non-polar solvents. Attention in the present publication is focused on the use of theory to predict the structure and properties of six 9-acridinones in excited S₁ and T₁ states in relation to those in the ground (S₀) state and to interpret the features of S₀ → S_n, S₀ → T₁, T₁ → T₂, S₁ → S₀, T₁ → S₀ and S₁ → T₁ transitions. We have also recorded absorption, fluorescence excitation and fluorescence spectra of these compounds, which provided us with the opportunity to compare our own and other available experimental information with that arising out of theoretical predictions.

2. Materials and methods

2.1. Chemicals

9(10*H*)-acridinone (99%) (**1**) was purchased from Sigma–Aldrich. 9(10-Methyl)-acridinone (**2**) was synthesized by the reaction of acridine with dimethyl sulphate [45]. 2-Methyl-9(10*H*)-acridinone was prepared following the method proposed by Drozdov [46]. Accordingly, 2-bromobenzoic acid was initially heated with *p*-toluidine in the presence of potassium carbonate. The product obtained was subsequently subjected to cyclization in the presence of POCl₃ to yield 2-methyl-9-acridinone. The final product, 2-methyl-9(10-methyl)-acridinone (**3**), was prepared by the reaction of 2-methyl-9-acridinone with dimethyl sulphate [47]. Nitration of **2** (at 100 °C) yielded a

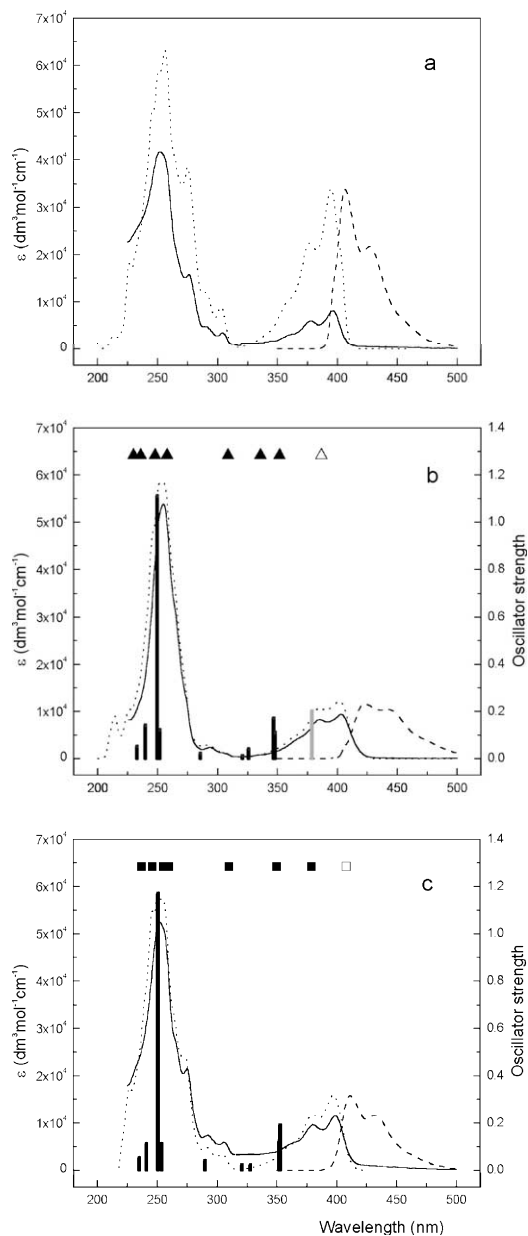


Fig. 3. Absorption (—), fluorescence excitation (····) and fluorescence (----) spectra of **2** in 1,4-dioxane (a), CH_3OH (b) and CH_3CN (c), together with theoretically predicted excitation (\blacksquare , \blacktriangle , \blacksquare) and emission (\square , \triangle , \square) transitions in the gaseous phase (b) and CH_3CN (c). PM3/S, lower values; PM3/CI, higher values.

mixture of the 2-nitro (85%) (**4**) and 4-nitro (15%) isomers, which were separated on the basis of solubility differences between the compounds in

hot acetic acid [48]. 9(10-Ethyl)-acridinone (**5**) was obtained in the reaction of **1** with iodoethane [49]. The first step in the synthesis of 9(10-phenyl)-acridinone (**6**) was the condensation of phenylamine with 2-bromobenzoic acid in the presence of powdered Cu as catalyst and potassium carbonate [46]. The 2-(*N*-phenylamino)benzoic acid product was then condensed with iodobenzene to yield 2-(*N,N*-diphenylamino)benzoic acid [49], the identity of which was confirmed by X-ray analysis [50]. The final product (**6**) was obtained by cyclizing the latter compound in the presence of sulphuric acid [51]. All substances were repeatedly recrystallized from ethanol before use. The purity of the compounds was verified by TLC and their chemical composition ascertained by elemental analysis and NMR spectroscopy [52].

2.2. Measurements

The absorption and steady-state fluorescence spectra were recorded on a Perkin–Elmer Lambda 18 spectrophotometer and LS-50 spectrofluorometer, respectively. The emission spectra were measured by adjusting the excitation wavelengths to the short-wavelength maxima in the absorption spectra, while fluorescence excitation spectra were recorded at wavelengths corresponding to the maxima in the emission spectra. Band intensity in the absorption spectra is given by ϵ (in $\text{dm}^3 \text{mol}^{-1} \text{cm}^{-1}$), while the intensities of fluorescence excitation and fluorescence spectra are in arbitrary units.

Spectral grade 1,4-dioxane, methyl alcohol and acetonitrile, all from Fluka, were used as solvents in all the spectroscopic measurements.

2.3. Quantum mechanical calculations

Unconstrained geometry optimizations of molecules (Fig. 1) in the ground (S_0) and excited singlet (S_1) or triplet (T_1) electronic states were carried out at the semi-empirical PM3 (S_0 state) and PM3/CI (S_1 or T_1 states) levels of theory [53], with standard procedures being employed together with the EF method [54,55] implemented in MOPAC 93 program package [56]. On completion of each optimization, the Hessian matrix was

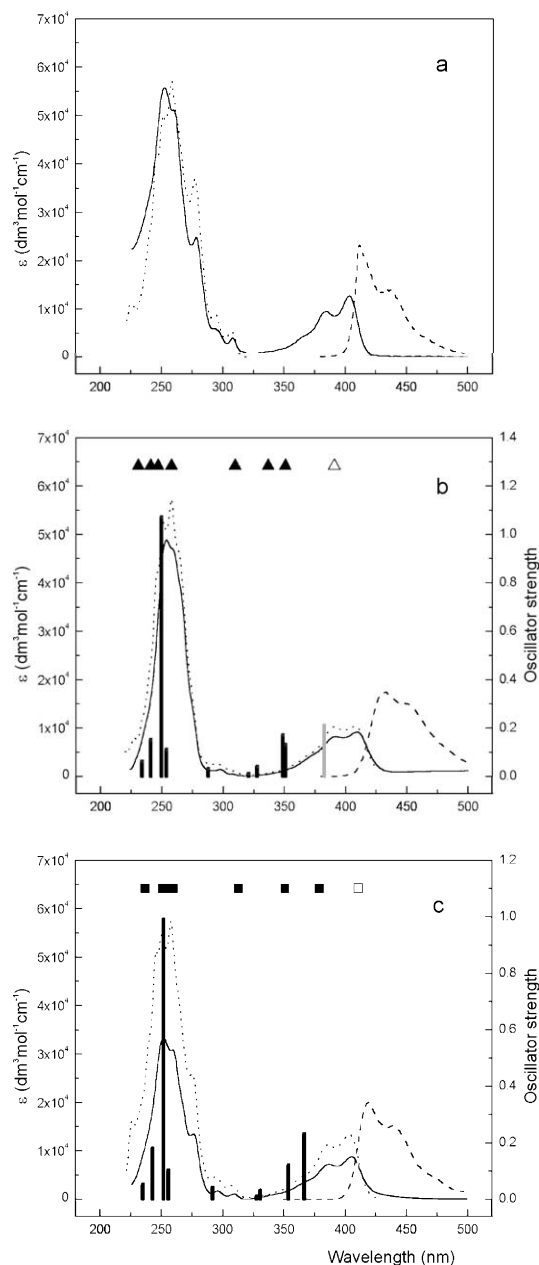


Fig. 4. Absorption (—), fluorescence excitation (····) and fluorescence (----) spectra of **3** in 1,4-dioxane (a), CH_3OH (b) and CH_3CN (c), together with theoretically predicted excitation (\blacksquare , \blacktriangle , \blacksquare) and emission (\square , \triangle , \square) transitions in the gaseous phase (b) and CH_3CN (c). PM3/S, lower values; PM3/CI, higher values.

calculated and verified for positive definiteness in order to assess whether or not the structures were

true minima [57]. The MOPAC 93 routines were then used to predict the thermochemical and physicochemical quantities for the compounds under investigation [56,57]. Solvent (1,4-dioxane, CH_3OH , CH_3CN) effects were included in the ground state geometry optimizations through the COSMO model [58]. The wavelengths of the electronic absorption transitions ($S_0 \rightarrow S_n$) were calculated either at PM3/CI [56] or PM3/S [59] levels using the ground state geometries. In the former case (PM3/CI), the ground and all excited state configurations, due to excitation within highest occupied (HOMO)–3 and lowest unoccupied (LUMO)+2 molecular orbitals, were included in the CI calculations. In the latter case (PM3/S), however, only the ground and single excited state configurations, due to excitation within the HOMO–6 and LUMO+6 molecular orbitals, were used [60]. Calculations at the PM3/S level also provided oscillator strengths [59]. In the prediction of electronic transitions, solvent effects were included at the PM3/CI level on the basis of the COSMO model [58]. The wavelengths of fluorescence ($S_1 \rightarrow S_0$), phosphorescence ($T_1 \rightarrow S_0$), singlet–triplet absorption ($S_0 \rightarrow T_1$), triplet–triplet absorption ($T_1 \rightarrow T_2$) and $S_1 \rightarrow T_1$ transitions (corresponding to the difference between the standard enthalpies of formation of triplet and singlet entities) were further predicted at the PM3/CI or PM3/S level using singlet (S_1) or triplet (T_1) geometries. The physicochemical characteristics of the compounds were extracted either directly from data files following geometry optimizations (HOMO and LUMO energies; dipole moments) or obtained with the available MOPAC 93 routines (bond orders [61], atomic partial charges [62]). All the characteristics were calculated with respect to ambient temperature and standard pressure.

3. Results and discussion

3.1. Experimental absorption and emission spectra

The absorption, fluorescence excitation and fluorescence spectra of the compounds investigated are presented in Figs. 2–7, together with the theoretically predicted absorption and fluores-

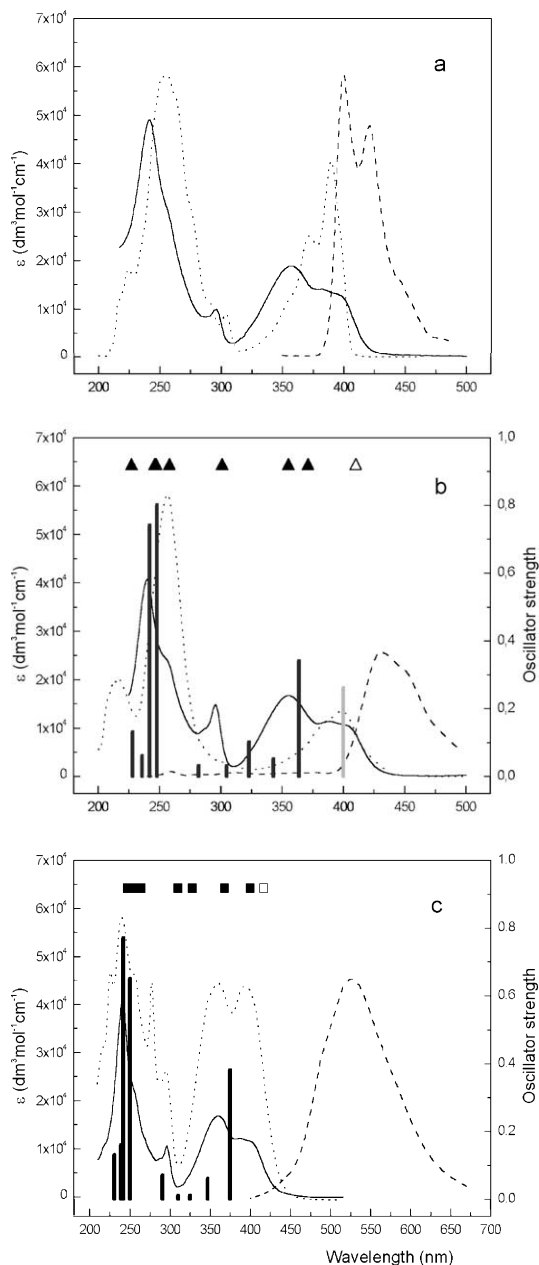


Fig. 5. Absorption (—), fluorescence excitation (·····) and fluorescence (----) spectra of **4** in 1,4-dioxane (a), CH₃OH (b) and CH₃CN (c), together with theoretically predicted excitation (■, ▲, ■) and emission (□, △, ▨) transitions in the gaseous phase (b) and CH₃CN (c). PM3/S, lower values; PM3/CI, higher values.

cence transitions. In general, our characteristics compare very well with those obtained by other

researchers [3–7,16,18,20,22]. The bands in the fluorescence excitation spectra are situated in the same wavelength region as those in the corresponding absorption spectra. However, the fluorescence excitation spectra sometimes display a more intricate structure than the corresponding absorption spectra, e.g. in the case of **1**, **5** or **6**. Furthermore, the maxima in the absorption and fluorescence excitation spectra of **4** appear at noticeably different wavelengths, which suggests that the solvation of molecules in the S₀ state may differ from that in the relaxed S₁ state.

Analysis of the spectra recorded in three solvents of different polarities, and of the ability of 9-acridinones to participate in H-bonding and electron-donor–acceptor interactions, revealed a number of regularities. To begin with, the absorption, fluorescence excitation and fluorescence bands always appeared at the highest wavelengths when the spectra were recorded in methanol and at the lowest wavelengths when measured in 1,4-dioxane. The corresponding bands in acetonitrile, which has the highest dielectric constant of the solvents used, lie in between the other two. Another feature is that the bands appearing around 300 nm always exhibit the highest intensity in the spectra recorded in 1,4-dioxane. A further regularity is that the spectra measured in methanol always contain fewer bands than those recorded in 1,4-dioxane or acetonitrile. These findings appear to indicate that 9-acridinones interact more readily with methanol molecules to form H-bonded complexes such as those postulated by Kokubun [6].

3.2. Theoretical versus experimental electronic absorption and emission transitions

To facilitate our interpretation of the spectra we calculated the wavelengths of the electronic transitions in 9-acridinones at the level of semi-empirical PM3/CI and PM3/S methods; the results are presented in Figs. 2–7 and Table 1. The wavelengths predicted by both methods for absorption transitions are always lower than those corresponding to the band maxima in the experimental spectra. For fluorescence, the theoretically predicted wavelengths of the emission transitions are also somewhat lower than the maxima of the

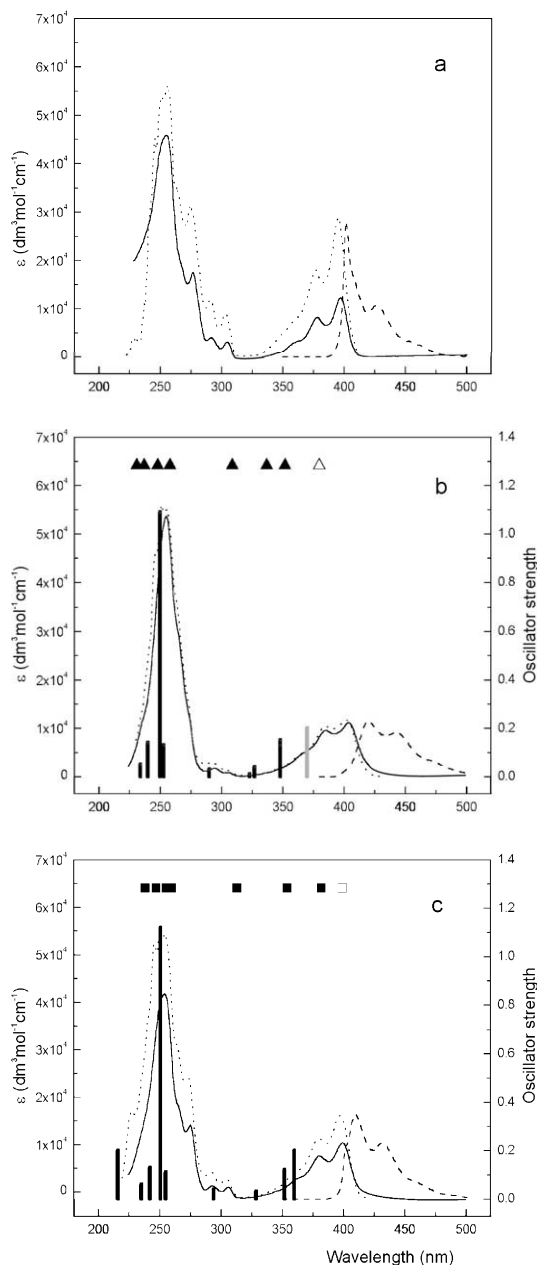


Fig. 6. Absorption (—), fluorescence excitation (·····) and fluorescence (----) spectra of **5** in 1,4-dioxane (a), CH_3OH (b) and CH_3CN (c), together with theoretically predicted excitation (\blacksquare , \blacktriangle , \blacksquare) and emission (\square , \triangle , \square) transitions in the gaseous phase (b) and CH_3CN (c). PM3/S, lower values; PM3/CI, higher values.

short-wavelength bands in the spectra, while in the case of phosphorescence the trend is reversed.

These findings suggest that the wavelengths of theoretically predicted transitions would better fit the experimental spectra if they were scaled, i.e. multiplied by certain factors. Such scaling factors for absorption transitions can be obtained by averaging the ratios of the wavelengths of long-wavelength bands in absorption (fluorescence excitation) spectra to those of the corresponding electronic transitions—both determined by us. In the case of absorption transition in CH_3CN , the respective scaling factors are 1.059 and 1.099 for data originating from the PM3/CI and PM3/S methods. The theoretically predicted wavelengths of $T_1 \rightarrow T_2$ transitions compare very well with the experimentally determined ones in the case of **1** and **5**, while for **2** the theoretically predicted wavelengths are somewhat lower than the empirical ones. The wavelengths of hypothetical $S_0 \rightarrow T_1$ transitions and the energy gap between the S_1 and T_1 states, given in Table 1, complete the information obtained by theoretical methods. Despite a certain inconsistency in the results, both theoretical methods provide quite good predictions of the electronic transition energies in 9-acridinones and facilitate the interpretation of experimental spectra.

3.3. Structure of electronically excited versus ground state molecules

The structures of the compounds investigated (Fig. 1) in the ground (S_0) and electronically excited (S_1 , T_1) states are presented in Fig. 8, while Table 2 sets out those structural parameters that change most markedly following the electronic excitation of 9-acridinones. As can be seen, excitation to the S_1 state increases the symmetry of **1** and lowers the symmetry of **2** and **6**, while excitation to the T_1 state lowers the symmetry of only **2**. In other cases, electronic excitation does not affect the symmetry. According to the results of theoretical calculations, 9(10*H*)-acridinone is non-planar in the S_0 and T_1 states but planar in the S_1 state. It is predicted that the other 9-acridinones investigated here are non-planar in all three electronic states. The C–C bond lengths of the lateral benzene rings in 9-acridinones ($C_{(1)}C_{(2)}/C_{(7)}C_{(8)}$) do not change substantially during elec-

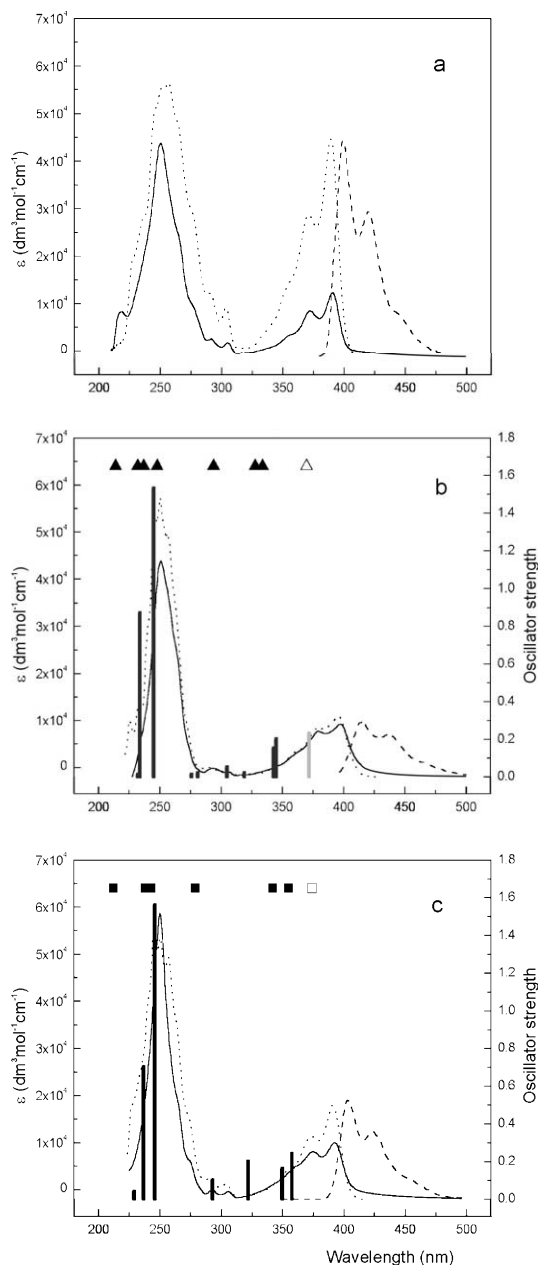


Fig. 7. Absorption (—), fluorescence excitation (·····) and fluorescence (----) spectra of **6** in 1,4-dioxane (a), CH_3OH (b) and CH_3CN (c), together with theoretically predicted excitation (\blacksquare , \blacktriangle , \blacksquare) and emission (\square , \triangle , \square) transitions in the gaseous phase (b) and CH_3CN (c). PM3/S, lower values; PM3/CI, higher values.

tronic excitation: inspection of the bond order values makes this immediately apparent. The same

applies to the N–C bonds of the central ring ($\text{N}_{(10)}\text{C}_{(12)}/\text{N}_{(10)}\text{C}_{(13)}$). It is interesting, however, that transformation of 9-acridinones from the S_0 to the S_1 or T_1 states alters the lengths of $\text{C}_{(1)}\text{C}_{(2)}/\text{C}_{(7)}\text{C}_{(8)}$ and $\text{N}_{(10)}\text{C}_{(12)}/\text{N}_{(10)}\text{C}_{(13)}$ bonds in **1**, **2**, **5** and **6**. The lengths of the $\text{C}_{(9)}\text{O}_{(15)}$ bond increase (and the bond orders correspondingly decrease) after excitation from the S_0 to the S_1 (more) or T_1 (less) states. An exception is the $S_0 \rightarrow T_1$ transition in **4**, during which the length of the $\text{C}_{(9)}\text{O}_{(15)}$ bond is reduced; the bond order increases correspondingly. Neither the $\text{N}_{(10)}$, $\text{C}_{(9)}$ and $\text{O}_{(15)}$, nor the $\text{C}_{(9)}$, $\text{N}_{(10)}$ and $\text{A}_{(16)}$ atoms are ever linear: electronic excitation alters the form of this non-linearity. The values of the dihedral angles indicate that the lateral benzene rings of 9-acridinones are only slightly non-planar in the ground and excited states. The central rings of the compounds are non-planar to a much greater degree, and this non-planarity changes as a result of electronic excitation. The considerable influence of solvents on the structure of the 9-acridinone ring system should also be noted: polar solvents (CH_3OH , CH_3CN) cause the central ring in the ground electronic state to flatten.

3.4. Properties of electronically excited versus ground state molecules

Basic thermodynamic ($\Delta_{f,298}H^\circ$, $_{298}S^\circ$) and physicochemical (HOMO and LUMO energies, dipole moments) characteristics of 9-acridinones in the ground (S_0) and excited (S_1 , T_1) states are given in Table 3. The standard enthalpies of formation of gaseous 9-acridinones are all positive: the lowest is for molecules in the S_0 state and the highest for those in the S_1 state. $\Delta_{f,298}H^\circ$ values for compounds in the T_1 state lie between the other two. Like standard enthalpies of formation, entropies are characteristic features of 9-acridinones, rising as the molecular masses of the compounds do so. In the case of 9(10*H*)-acridinone, the value of $_{298}S^\circ$ is highest when the molecules are in the S_0 state, lower when they are in the S_1 state, and lowest when they are in the T_1 state.

According to Koopman's theorem, the negative energies of LUMO and HOMO (Table 3), respectively, approximate the electron affinity and the

Table 1

Singlet–triplet ($S_0 \rightarrow T_1$) and triplet–triplet ($T_1 \rightarrow T_2$) absorption transitions, singlet–singlet ($S_1 \rightarrow S_0$) phosphorescence transitions and singlet–triplet ($S_1 \rightarrow T_1$) energy gaps in 9-acridinones (nm)

Compound	Method	Solvent	Transition (energy gap)				Refs.		
			$S_0 \rightarrow T_1$	$T_1 \rightarrow T_2$	$S_1 \rightarrow S_0$	$S_1 \rightarrow T_1$			
1	Experimental	Ethanol		575			[41]		
		Ethanol (77 K)			475		[20,22]		
		Methylcyclohexane/ 2-methylbutane (77 K)			491		[20]		
	PM3/CI	CH ₃ CN		448	572	561	908		
				499	573	565			
PM3/S	CH ₃ CN		477		621				
2	Experimental	Cyclohexane		640			[42]		
		1,4-Dioxane		625			[42]		
		Benzene		630			[17]		
				640			[42]		
		CHCl ₃		623			[42]		
		2-Propanol		590			[17]		
		Acetone		615			[42]		
		CH ₃ OH		582			[42]		
		CH ₃ CN		610			[42]		
		H ₂ O+ethanol		570			[17]		
		Ethanol (77 K)				475		[20,22]	
		Methylcyclohexane/ 2-methylbutane (77 K)				485		[20]	
		PM3/CI	CH ₃ CN		451	580	565	926	
	494			581	573				
PM3/S	CH ₃ CN		478		611				
3	PM3/CI	CH ₃ CN		456	580	566	959		
				499	583	574			
PM3/S	CH ₃ CN		483		644				
4	PM3/CI	CH ₃ CN		457	558	553	992		
				482	549	541			
PM3/S	CH ₃ CN		494		613				
5	Experimental	Ethanol		580			[22,26]		
		Ethanol (77 K)			475		[22]		
		PM3/CI	CH ₃ CN	500	569	557	915		
PM3/S	CH ₃ CN		478		605				
6	Experimental	Ethanol (77 K)			471		[20]		
		Ethanol (72 K)			475		[22]		
		Methylcyclohexane/ 2-methylbutane (77 K)			489		[20]		
		PM3/CI	CH ₃ CN		414	516	513	926	
					436	504	504		
PM3/S	CH ₃ CN		465		547				

first ionization potential of a molecule [64]. The ionization potentials (in eV) of 9(10*H*)-acridinone (7.60 [65] or 7.69 [66]), 9(10-methyl)-acridinone (7.53 [65]), 9(10-ethyl)-acridinone (7.49 [65]) and

9(10-phenyl)-acridinone (7.46 [65]) are on average 0.974 eV lower than negative HOMO energies. This value can thus be used to correct the ionization potentials of 9-acridinones in the

Table 2

Structural characteristics of 9-acridinones in the ground (S_0) and excited (S_1 , T_1) electronic states predicted at the PM3 (PM3-COSMO) (S_0) or PM3/CI (S_1 , T_1) levels of theory

Compound (Fig. 1)	Medium	Bond lengths ^a			Bond orders			Angle	Dihedral angles ^a		
		C ₍₁₎ C ₍₂₎ / C ₍₇₎ C ₍₈₎	C ₍₉₎ O ₍₁₅₎	N ₍₁₀₎ C ₍₁₂₎ / N ₍₁₀₎ C ₍₁₃₎	C ₍₁₎ C ₍₂₎ / C ₍₇₎ C ₍₈₎	C ₍₉₎ O ₍₁₅₎	N ₍₁₀₎ C ₍₁₂₎ / N ₍₁₀₎ C ₍₁₃₎		N ₍₁₀₎ C ₍₉₎ O ₍₁₅₎ / C ₍₉₎ N ₍₁₀₎ A ₍₁₆₎	C ₍₃₎ C ₍₂₎ C ₍₁₎ C ₍₁₁₎ / C ₍₆₎ C ₍₇₎ C ₍₈₎ C ₍₁₄₎	C ₍₁₁₎ C ₍₁₂₎ N ₍₁₀₎ C ₍₁₃₎ / C ₍₁₂₎ N ₍₁₀₎ C ₍₁₃₎ C ₍₁₄₎
<i>S₀ state</i>											
1	Gaseous	1.39	1.22	1.42	1.46	1.86	1.09	170/170	0	−19/19	10/−10
	1,4-Di-oxane	1.39	1.23	1.42	1.46	1.85	1.09	170/161	0	−19/19	10/−10
	CH ₃ OH	1.38	1.24	1.41	1.48	1.83	1.10	173/165	0	−15/15	6/−6
	CH ₃ CN	1.38	1.24	1.41	1.48	1.83	1.10	173/165	0	−15/15	6/−6
2	Gaseous	1.39	1.22	1.43	1.46	1.85	1.07	177/160	0	−9/9	2/−2
	1,4-Di-oxane	1.38	1.23	1.43	1.46	1.85	1.07	177/161	0	−9/9	2/−2
	CH ₃ OH	1.38	1.24	1.42	1.48	1.83	1.08	178/164	0	−7/7	0
	CH ₃ CN	1.38	1.24	1.42	1.48	1.83	1.08	178/164	0	−7/7	0
3	Gaseous	1.39	1.22	1.43	1.44/ 1.46	1.85	1.07	177/160	0	−9/9	2/−2
	1,4-Di-oxane	1.39/ 1.38	1.23	1.43	1.45/ 1.46	1.85	1.07	177/160	0	−9/9	1/−1
	CH ₃ OH	1.39/ 1.38	1.24	1.42	1.46/ 1.48	1.83	1.08/1.09	178/164	0	−7/7	1/−1
	CH ₃ CN	1.39/ 1.38	1.24	1.42	1.46/ 1.48	1.83	1.08/1.09	178/164	0	−7/7	1/−1
4	Gaseous	1.40/ 1.39	1.22	1.42/1.43	1.40/ 1.46	1.86	1.13/1.06	177/165	0	−8/7	1/−2
	1,4-Di-oxane	1.40/ 1.39	1.23	1.41/1.43	1.40/ 1.46	1.86	1.14/1.06	179/166	0	−6/5	0
	CH ₃ OH	1.40/ 1.38	1.24	1.40/1.43	1.41/ 1.47	1.84	1.18/1.07	178/173	0	−1/2	3/−3
	CH ₃ CN	1.40/ 1.38	1.24	1.40/1.43	1.41/ 1.47	1.84	1.17/1.07	179/173	0	−1/1	2/−2
5	Gaseous	1.39	1.22	1.43	1.46	1.85	1.07	178/157	0	3/−3	4/−4
	1,4-Di-oxane	1.38	1.23	1.43	1.47	1.85	1.07	178/158	0	3/−3	5/−5
	CH ₃ OH	1.38	1.24	1.42	1.48	1.83	1.09	177/162	0	2/−2	5/−5
	CH ₃ CN	1.38	1.24	1.42	1.48	1.83	1.08	178/163	0	3/−3	4/−4
6	Gaseous	1.39	1.22	1.43	1.46	1.85	1.07	173/167	0	−14/14	6/−6

Table 2 (Continued)

Compound (Fig. 1)	Medium	Bond lengths ^a			Bond orders			Angle	Dihedral angles ^a		
		C ₍₁₎ C ₍₂₎ / C ₍₇₎ C ₍₈₎	C ₍₉₎ O ₍₁₅₎	N ₍₁₀₎ C ₍₁₂₎ / N ₍₁₀₎ C ₍₁₃₎	C ₍₁₎ C ₍₂₎ / C ₍₇₎ C ₍₈₎	C ₍₉₎ O ₍₁₅₎	N ₍₁₀₎ C ₍₁₂₎ / N ₍₁₀₎ C ₍₁₃₎		N ₍₁₀₎ C ₍₉₎ O ₍₁₅₎ / C ₍₉₎ N ₍₁₀₎ A ₍₁₆₎	C ₍₃₎ C ₍₂₎ C ₍₁₎ C ₍₁₁₎ / C ₍₆₎ C ₍₇₎ C ₍₈₎ C ₍₁₄₎	C ₍₁₁₎ C ₍₁₂₎ N ₍₁₀₎ C ₍₁₃₎ / C ₍₁₂₎ N ₍₁₀₎ C ₍₁₃₎ C ₍₁₄₎
	1,4-Di-oxane	1.38	1.23	1.43	1.47	1.84	1.07	173/169	0	-14/14	7/-7
	CH ₃ OH	1.38	1.24	1.41	1.48	1.82	1.10	179	0	-2/2	1/-1
	CH ₃ CN	1.38	1.24	1.41	1.48	1.82	1.10	179	0	-1/1	0
<i>S₁ state</i>											
1	Gaseous	1.39/ 1.38	1.23	1.39/1.42	1.34/ 1.52	1.73	1.25/1.18	177/180	0	0	0
2	Gaseous	1.40/ 1.38	1.23	1.39/1.44	1.34/ 1.52	1.72	1.22/1.13	172/166	1/-1	-9/17	11/-3
3	Gaseous	1.40/ 1.38	1.23	1.39/1.44	1.30/ 1.53	1.71	1.24/1.12	172/164	1/-1	-9/17	10/-2
4	Gaseous	1.38	1.23	1.47/1.39	1.39/ 1.38	1.81	1.08/1.28	170/157	0/-1	-25/11	1/-14
5	Gaseous	1.38/ 1.40	1.23	1.43/1.40	1.52/ 1.34	1.71	1.14/1.22	172/170	1	-12/12	9/-9
6	Gaseous	1.38/ 1.40	1.23	1.43/1.39	1.51/ 1.34	1.72	1.14/1.22	175/170	1/-1	-14/5	-2/-7
<i>T₁ state</i>											
1	Gaseous	1.38/ 1.37	1.23	1.44/1.38	1.40/ 1.52	1.75	1.10/1.22	173/165	0	-15/15	7/-7
2	Gaseous	1.38/ 1.37	1.23	1.45/1.39	1.41/ 1.54	1.73	1.09/1.19	177/159	0/1	3/-7	-3/-1
3	Gaseous	1.39/ 1.37	1.23	1.45/1.39	1.39/ 1.54	1.73	1.09/1.19	177/158	1	4/-7	-3/0
4	Gaseous	1.43/ 1.39	1.22	1.39/1.45	1.18/ 1.40	1.88	1.19/1.11	170/154	1/0	-10/10	12/-12
5	Gaseous	1.37/ 1.38	1.23	1.39/1.45	1.54/ 1.40	1.73	1.20/1.08	175/159	1	-5/7	8/-6
6	Gaseous	1.37/ 1.38	1.23	1.39/1.45	1.53/ 1.40	1.73	1.19/1.09	178/164	0	0/2	3/-1

Bond lengths are in Å and bond angles in degrees; bond orders originate from rotationally invariant bond order analysis [61].

^a The values for the gaseous medium (*S*₀ state) were taken from our previous work [63].

ground electronic state. The HOMO energies of 9-acridinones in the S_1 and T_1 states are comparable, but much higher than those in the S_0 state. This means that the ionization of such molecules would require much less energy. The negative LUMO energies are unexpected: this suggests that following electron attachment, 9-acridinones form stable negative ions in both ground (S_0) and excited (S_1 , T_1) states. As this characteristic was not confirmed experimentally, we do not think that the predicted

LUMO energies are very reliable. These energies of gaseous 9-acridinones are quite similar in the ground and excited electronic states; however, these quantities are lower in polar solvents.

Dipole moments (μ) are a reflection of non-uniform negative charge distribution within molecules. The dipole moments (in D), measured in benzene, of 9(10*H*)-acridinone (6.0 [20]), 9(10-methyl)-acridinone (5.3 [20] or 5.39 [67]), and 9(10-phenyl)-acridinone (5.4 [20]) compare reason-

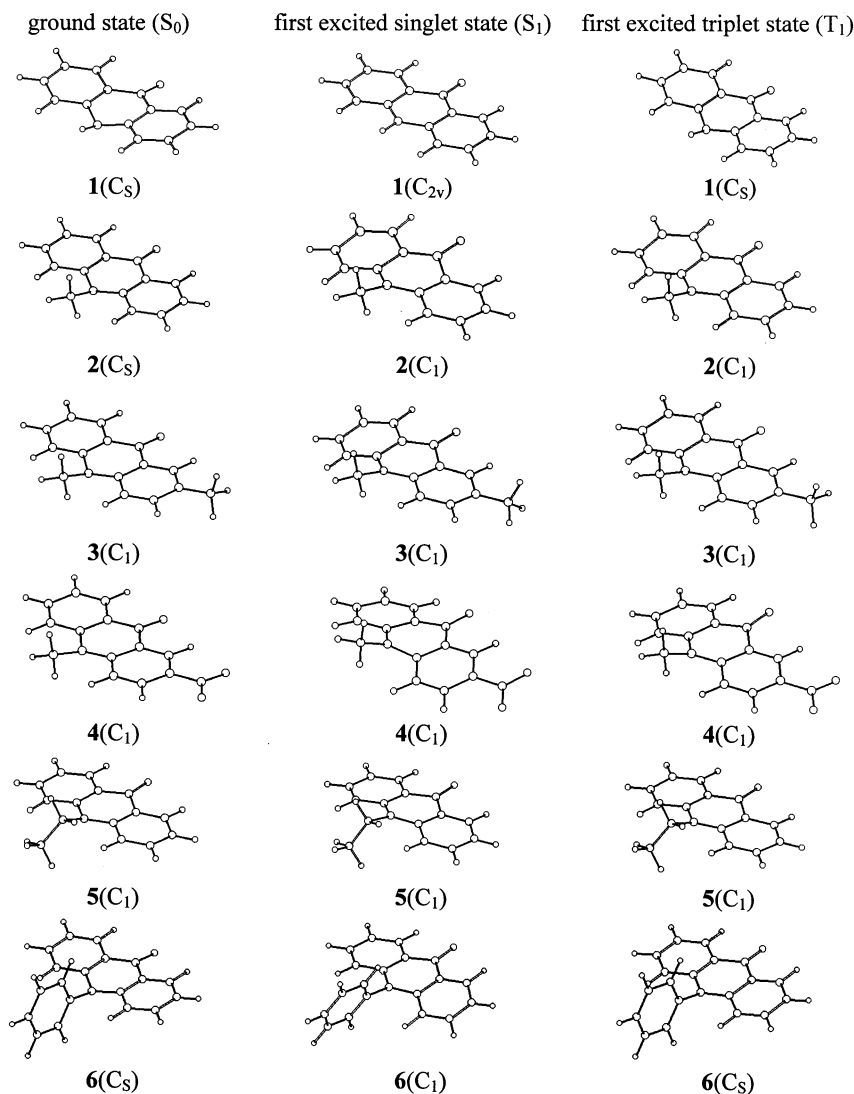


Fig. 8. PM3 (the ground (S_0) state) and PM3/CI (the excited (S_1 , T_1) electronic states) optimized geometries of 9-acridinones (the point group symmetry is indicated in parentheses following the numbering of molecules).

Table 3

Physicochemical characteristics of 9-acridinones in the ground (S_0) and excited (S_1 , T_1) electronic states predicted at the PM3 (PM3-COSMO) (S_0) or PM3/CI (S_1 , T_1) levels of theory

Compound (Fig. 1)	Medium	$\Delta_{f,298}H^{\circ a}$	${}_{298}S^{\circ a}$	Energy		μ	Relative atomic charge						
				HOMO	LUMO		$C_{(9)}$	$N_{(10)}$	$O_{(15)}$				
<i>S₀ state</i>													
1	Gaseous	57	428	-8.5	-0.6	3.8	0.39	0.18	-0.34				
	1,4-Dioxane	39		-8.6	-0.7					4.7	0.43	0.18	-0.40
	CH ₃ OH	11		-8.6	-0.9					7.0	0.47	0.22	-0.51
	CH ₃ CN	11		-8.6	-0.9					7.0	0.47	0.22	-0.51
2	Gaseous	65	459	-8.4	-0.6	4.0	0.39	0.15	-0.34				
	1,4-Dioxane	48		-8.5	-0.7					4.9	0.42	0.16	-0.40
	CH ₃ OH	22		-8.6	-1.0					7.0	0.47	0.19	-0.51
	CH ₃ CN	22		-8.6	-1.0					7.1	0.47	0.19	-0.51
3	Gaseous	26	505	-8.4	-0.6	3.9	0.39	0.16	-0.34				
	1,4-Dioxane	9		-8.4	-0.7					4.8	0.42	0.16	-0.40
	CH ₃ OH	-17		-8.5	-1.0					6.9	0.47	0.19	-0.51
	CH ₃ CN	-17		-8.5	-1.0					7.0	0.47	0.19	-0.51
4	Gaseous	27	527	-9.0	-1.3	8.9	0.39	0.18	-0.33				
	1,4-Dioxane	-23		-9.0	-1.3					10.5	0.42	0.19	-0.39
	CH ₃ OH	-96		-8.7	-1.3					13.8	0.48	0.25	-0.50
	CH ₃ CN	-97		-8.7	-1.3					13.9	0.48	0.25	-0.50
5	Gaseous	40	460	-8.4	-0.6	4.1	0.39	0.14	-0.34				
	1,4-Dioxane	23		-8.5	-0.7					5.0	0.42	0.15	-0.40
	CH ₃ OH	2		-8.6	-1.0					7.1	0.47	0.17	-0.51
	CH ₃ CN	-3		-8.6	-1.0					7.1	0.47	0.17	-0.51
6	Gaseous	200	536	-8.4	-0.5	4.7	0.39	0.22	-0.34				
	1,4-Dioxane	182		-8.5	-0.7					5.6	0.42	0.23	-0.40
	CH ₃ OH	156		-8.5	-1.0					7.9	0.47	0.28	-0.51
	CH ₃ CN	155		-8.5	-1.0					7.9	0.47	0.27	-0.51
<i>S₁ state</i>													
1	Gaseous	431	401	-2.8	-0.4	4.0	0.32	0.51	-0.32				
2	Gaseous	434		-2.7	-0.4					4.3	0.31	0.47	-0.32
3	Gaseous	391		-2.6	-0.4					4.2	0.31	0.46	-0.32
4	Gaseous	377		-3.5	-1.1					10.0	0.36	0.49	-0.28
5	Gaseous	415		-2.7	-0.4					4.5	0.31	0.46	-0.32
6	Gaseous	570		-2.7	-0.8					4.5	0.31	0.56	-0.32
<i>T₁ state</i>													
1	Gaseous	299	394	-2.9	-0.4	4.8	0.32	0.46	-0.34				
2	Gaseous	304		-2.9	-0.4					5.5	0.31	0.44	-0.35
3	Gaseous	266		-2.8	-0.4					5.5	0.30	0.45	-0.35
4	Gaseous	257		-3.6	-1.1					12.2	0.36	0.49	-0.29
5	Gaseous	284		-2.8	-0.4					5.6	0.30	0.44	-0.35
6	Gaseous	440		-2.8	-0.6					6.3	0.31	0.51	-0.35

$\Delta_{f,298}H^{\circ}$ (kJ mol⁻¹) denotes the standard enthalpy of formation; ${}_{298}S^{\circ}$ (J mol⁻¹ K⁻¹) is the entropy; HOMO and LUMO (eV) indicate the energies of the HOMO and LUMO; μ , in Debyes (1 Debye = 3.336 × 10⁻³⁰ Cm), is the dipole moment; relative atomic charges are derived from Mulliken population analysis [62].

^a Values for the gaseous medium (S_0 state) were taken from our previous work [63].

ably well with those predicted at the PM3 level in 1,4-dioxane. Compound **4** can be regarded as highly polar, since its dipole moment is relatively

high; this quantity is smaller in the less-polar 9-acridinones, i.e. **1**, **2**, **3**, **5** and **6**. The theoretical value of a dipole moment depends substantially on

the solvent in which it is measured and increases as its polarity does so. On comparing predicted μ values of gaseous 9-acridinones, the following sequence can be noted: $\mu(T_1) > \mu(S_1) > \mu(S_0)$. Abdullah and Kemp reported a value of $\mu(T_n)$ for 9(10-methyl)-acridinone equal to 5.85 D [42], which corresponds quite well to the value of 5.46 D predicted at the PM3/CI level. On the other hand, the value of μ of 7.287 D for this compound in the S_1 state reported by Koutek [67] is much higher than that predicted at the PM3/CI level and seems to have been overestimated. Dipole moments may be considered a measure of the ability of 9-acridinones in various electronic states to participate in non-specific interactions with other molecules. The data in Table 3 can thus serve as a convenient source of information enabling the features of such interactions to be predicted.

3.5. Electron density changes accompanying electronic excitation

The theoretically predicted changes of dipole moments caused by electronic excitation (Table 3)

indicate that the process is accompanied by changes in electron density distribution. This effect is demonstrated directly in Fig. 9 and in Table 3, where the relative atomic charges on selected atoms are given. Theory predicts that the principal changes in electron density accompanying the $S_0 \rightarrow S_1$ and $T_1 \rightarrow S_0$ transitions occur within the heterocyclic N atom and the adjacent C atom (Fig. 9). Furthermore, changes in electron density occur in one of the lateral benzene rings containing this C atom. The keto group, and the substituents in positions 2 and 10, participate only slightly in the electronic transitions within the ground and excited states. Atomic charges are a quantitative reflection of electron density changes; these values for $C_{(9)}$, $N_{(10)}$ and $O_{(15)}$ atoms are given in Table 3. Theory predicts that there is always a negative charge deficiency at the $C_{(9)}$ and $N_{(10)}$ atoms and an excess of negative charge at the $O_{(15)}$ atom (oxygen is the most electronegative of the elements present in 9-acridinones). The atomic charges change slightly at the $C_{(9)}$ and $O_{(15)}$ atoms and substantially at the $N_{(10)}$ atom following electronic excitation, which is demonstrated directly in Fig.

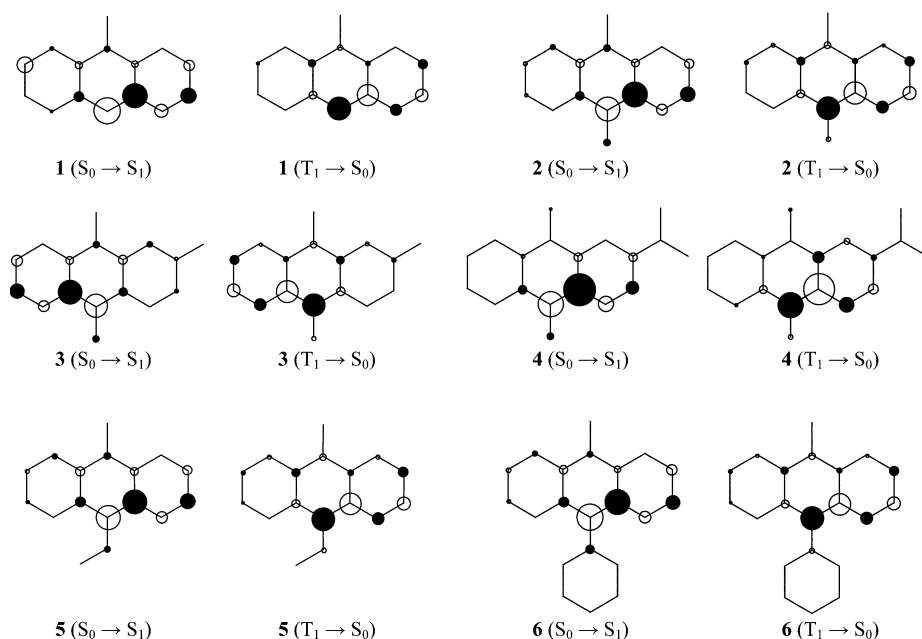


Fig. 9. Changes in electron densities accompanying $S_0 \rightarrow S_1$ and $T_1 \rightarrow S_0$ transitions in 9-acridinones. Empty circles indicate the decrease and filled circles the increase of the electron density at a given atom; the area of the circles is proportional to the absolute value of the electron density change at a given atom.

9. Without doubt, the electron density changes (Fig. 9) indicate that the electronic transitions must be accompanied by dipole moment changes—an effect predicted by theory (Table 3) and proven experimentally [42].

4. Concluding remarks

These investigations have provided the absorption and fluorescence characteristics of the basic form of 9(10*H*)-acridinone and five of its derivatives, which were selected in such a way as to reveal the influence of different substituents on the spectral features of this group of compounds. Three solvents with different polarities and abilities to participate in H-bonding and electron-donor–acceptor interactions were used in the spectral measurements and calculations in order to examine how a medium's properties can affect spectral characteristics. The experimental data obtained by us and others [3–7,16–18,20,22,26,41,42] were subsequently compared with the characteristics predicted by us, in order to verify the extent to which theory approximates experimental results. Moreover, the calculations provided numerous, experimentally unavailable, characteristics of the compounds in excited states. Our investigations have thus added to the information on the electron spectroscopy of 9-acridinones, light-emitting compounds which are formed upon electronic excitation of parent molecules or during the oxidation of acridinium entities, and provide insight into the nature of the electronic transitions occurring in them. The information gathered in this work therefore supplies a convenient framework within which to consider the electron spectroscopy of 9-acridinones and may be useful in designing fluorescent or chemiluminescent indicators or labels with potentially interesting applications.

Acknowledgements

The authors acknowledge the financial support of Polish State Committee for Scientific Research

(KBN) under grant 3 T09A 083 16 (contract No. 1177/T09/99/16).

References

- [1] A. Albert, *The Acridines*, 2nd ed., Edward Arnold, London, 1966.
- [2] R.M. Acheson (Ed.), *Acridines*, 2nd ed., Interscience, New York, 1973.
- [3] P. Beak, F.S. Fry, J. Lee, F. Stelle, *J. Am. Chem. Soc.* 98 (1976) 171.
- [4] A. Albert, L.N. Short, *J. Chem. Soc.* (1945) 760.
- [5] R.M. Acheson, M.L. Burstall, C.W. Jefford, B.F. Sansom, *J. Chem. Soc.* (1954) 3742.
- [6] H. Kokubun, *Z. Elektrochem.* 62 (1958) 599.
- [7] V. Zanker, A. Wittwer, *Z. Phys. Chem. (N.F.)* 24 (1960) 183.
- [8] V.P. Maksimets, A.K. Sukhomlinov, *Khim. Geterotsikl. Soedin.* (1966) 739.
- [9] V. Zanker, E. Cmiel, *Liebigs Ann. Chem.* (1975) 1576.
- [10] F. Fushimi, K. Kikuchi, H. Kokubun, *J. Photochem.* 5 (1976) 457.
- [11] S.M. Bendig, *Z. Naturforsch. A* 35 (1980) 1076.
- [12] T.V. Sakhno, G.A. Val'kova, S.N. Shcherbo, D.N. Shigorin, *Zh. Fiz. Khim.* 57 (1983) 694.
- [13] M. Siegmund, J. Bendig, M. Loewis of Menar, J. Wilda, *Monatsh. Chem.* 117 (1986) 1113.
- [14] Z. Gryczynski, A. Kawski, *Acta Phys. Pol. A* 70 (1986) 105.
- [15] E.H. White, D.F. Roswell, A.C. Dupont, A.A. Wilson, *J. Am. Chem. Soc.* 109 (1987) 5189.
- [16] S. Niizuma, H. Kawata, *Bull. Chem. Soc. Jpn.* 66 (1993) 1627.
- [17] H. Kawata, S. Niizuma, *J. Prakt. Chem.* 336 (1994) 425.
- [18] H. Kokubun, *Z. Phys. Chem. (N.F.)* 101 (1976) 137.
- [19] F. Calardin, *Z. Phys. Chem. (N.F.)* 106 (1977) 25.
- [20] M. Siegmund, J. Bendig, *Ber. Bunsen-Ges. Phys. Chem.* 82 (1978) 1061.
- [21] G.A. Val'kova, S.N. Shcherbo, D.N. Shigorin, *Dokl. Akad. Nauk. SSSR* 240 (1978) 884.
- [22] S.N. Shcherbo, G.A. Val'kova, D.N. Shigorin, R.S. Sorokina, L.F. Rybakova, *Zh. Fiz. Khim.* 53 (1979) 562.
- [23] S.G. Schulman, W.J.M. Underberg, *Anal. Chim. Acta* 107 (1979) 411.
- [24] J. Bendig, M. Siegmund, A. Kawski, *Z. Chem.* 20 (1980) 216.
- [25] J. Bendig, M. Siegmund, *Z. Phys. Chem.* 262 (1981) 834.
- [26] S.N. Shcherbo, G.A. Val'kova, D.N. Shigorin, *Zh. Fiz. Khim.* 55 (1981) 795.
- [27] T.V. Sakhno, G.G. Konoplev, G.A. Val'kova, D.N. Shigorin, *Zh. Fiz. Khim.* 56 (1982) 878.
- [28] M. Siegmund, J. Bendig, J. Wilda, K. Teuchner, *Z. Chem.* 25 (1985) 372.

- [29] G.A. Val'kova, N.A. Rudenko, R.S. Sorokina, L.F. Rybakova, A.N. Poplavskii, *Zh. Fiz. Khim.* 62 (1988) 1032.
- [30] S.N. Shcherbo, G.A. Val'kova, I.V. Savchenko, D.N. Shigorin, *Zh. Fiz. Khim.* 62 (1988) 2266.
- [31] S.N. Shcherbo, I.V. Savchenko, G.A. Val'kova, D.N. Shigorin, *Zh. Fiz. Khim.* 62 (1988) 2269.
- [32] G.A. Val'kova, N.V. Korol'kova, M.B. Ryzhikov, A.N. Rodionov, A.I. Raznoshinskii, V.I. Jushkov, S.N. Shcherbo, D.N. Shigorin, *Zh. Fiz. Khim.* 65 (1991) 1227.
- [33] I.V. Korotkova, T.V. Sakhno, V.V. Solov'ev, *Ukr. Khim. Zh. (Russ. Ed.)* 64 (1998) 81.
- [34] P. Nikolov, I. Petkova, G. Koehler, S. Stojanov, *J. Mol. Struct.* 448 (1998) 247.
- [35] M.M. Rauhut, D. Sheenan, R.A. Clarke, B.G. Roberts, A.M. Semsel, *J. Org. Chem.* 30 (1965) 3587.
- [36] E. Rapaport, M.W. Cass, E.H. White, *J. Am. Chem. Soc.* 94 (1972) 3160.
- [37] M.W. Cass, E. Rapaport, E.H. White, *J. Am. Chem. Soc.* 94 (1972) 3168.
- [38] I. Kamiya, T. Sugimoto, K. Yamabe, *Bull. Chem. Soc. Jpn.* 57 (1984) 1735.
- [39] J. Stauff, G. Stark, *Z. Naturforsch. B* 41 (1986) 113.
- [40] K. Sakanishi, Y. Kato, E. Mizukoshi, K. Shimizu, *Tetrahedron Lett.* 35 (1994) 4789.
- [41] Y. Miyashita, S. Niizuma, H. Kokubun, M. Koizumi, *Bull. Chem. Soc. Jpn.* 46 (1973) 3373.
- [42] K.A. Abdullah, T.J. Kemp, *J. Photochem.* 32 (1986) 49.
- [43] S. Ishijima, M. Higashi, H. Yamaguchi, *J. Phys. Chem.* 98 (1994) 10432.
- [44] T.V. Sakhno, I.V. Korotkova, T.P. Shcherban, *Ukr. Khim. Zh. (Russ. Ed.)* 64 (1998) 110.
- [45] C. Graebe, K. Lagodzinski, *Liebigs Ann. Chem.* 276 (1893) 35.
- [46] N.S. Drozdov, *J. Gen. Chem. (USSR)* 7 (1937) 2292[*Chem. Abstr.* 32 (1938) 568].
- [47] I.D. Postescu, D. Suci, *J. Prakt. Chem.* 318 (1976) 515.
- [48] K. Lehmstedt, H. Hundertmark, *Chem. Ber.* 64 (1931) 2386.
- [49] I. Goldberg, M. Nimerovsky, *Chem. Ber.* 40 (1907) 2448.
- [50] A. Bouzyk, A. Konitz, J. Blazejowski, *Acta Crystallogr. C* 57 (2001) 985.
- [51] C. Graebe, K. Lagodzinski, *Chem. Ber.* 25 (1892) 1733.
- [52] A. Bouzyk, L. Jozwiak, J. Blazejowski, *J. Mol. Struct.* 612 (2002) 29.
- [53] J.J.P. Stewart, *J. Comput. Chem.* 10 (1989) 209, 221.
- [54] J. Baker, *J. Comput. Chem.* 7 (1986) 385.
- [55] J. Baker, *J. Comput. Chem.* 9 (1988) 465.
- [56] J.J.P. Stewart, *MOPAC 93*, Copyright Fujitsu, Tokyo, Japan, 1993.
- [57] J.J.P. Stewart, *J. Comput.-Aided Mol. Des.* 4 (1990) 1.
- [58] A. Klamt, G.Z. Schurmann, *J. Chem. Soc. Perkin Trans. 2* (1993) 799.
- [59] HyperChem 5.0, Hypercube Inc., Waterloo, ON, Canada, 1995.
- [60] D.R. Armstrong, P.G. Perkins, J.J.P. Stewart, *J. Chem. Soc. Faraday Trans. 2* 68 (1972) 1839.
- [61] D.R. Armstrong, P.G. Perkins, J.J.P. Stewart, *J. Chem. Soc. Dalton Trans.* (1973) 838.
- [62] R.S. Mulliken, *J. Chem. Phys.* 23 (1955) 1833, 1841.
- [63] A. Bouzyk, L. Jozwiak, A. Wroblewska, J. Rak, J. Blazejowski, *J. Phys. Chem. A* 106 (2002) 3957.
- [64] T. Koopmans, *Physica* 1 (1934) 104.
- [65] V.K. Potapov, A.D. Filyugina, D.N. Shigorin, G.A. Ozerova, *Dokl. Akad. Nauk. SSSR* 180 (1968) 398.
- [66] S. Ishijima, M. Higashi, H. Yamaguchi, M. Kubota, T. Kobayashi, *J. Electron Spectrosc. Relat. Phenom.* 82 (1996) 71.
- [67] B. Koutek, *Collect. Czech. Chem. Commun.* 49 (1984) 1680.